PAPER

NJC
www.rsc.org/njc

# Cation-reinforced donor-acceptor pseudorotaxanes

**Sofia I. Pascu, Thibaut Jarrosson, Christoph Naumann, Sijbren Otto, Guido Kaiser and Jeremy K. M. Sanders***

*Department of Chemistry, University of Cambridge, Lensfield Road, Cambridge, UK CB2 1EW. E-mail: jkms@cam.ac.uk*

***Received (in Montpellier, France) 4th October 2004, Accepted 17th November 2004***
***First published as an Advance Article on the web 15th December 2004***



Formation of a series of pseudorotaxanes from an electron-rich crown ether (host **1**), pyromellitic diimide (guest **2**) and alkali salt templates MX, where M = $Li^+$ and $Na^+$, and $X^-$ = $Br^-$, $I^-$, $CF_3SO_3^-$, $[B(C_6F_5)_4]^-$ and $[B\{3,5\text{-}(CF_3)_2(C_6H_3)\}_4]^-$, is reported. Mixing of **1** and **2** in $CH_2Cl_2$ or a mixture of $CHCl_3$ and MeOH (98 : 2) gave a pale yellow solution indicative of a very weak charge-transfer interaction. Upon addition of MX, brightly coloured solutions were obtained, resulting from a red shift and an increase in the intensity of the charge-transfer band. Structural and kinetic studies of the pseudorotaxanes were performed by NMR. The solution-phase structures of $[M_2 \cdot \mathbf{1} \cdot \mathbf{2}]^{2+}$ are in good agreement with the solid-phase structure determined by X-ray crystallography. The remarkable templating properties of $Li^+$ for the $\mathbf{1} \cdot \mathbf{2}$ donor-acceptor complex are due to the almost perfect coincidence of coordinative geometries in $[Li_2 \cdot \mathbf{1}]^{2+}$ and $[Li_2 \cdot \mathbf{1} \cdot \mathbf{2}]^{2+}$.

## Introduction

Recent years have seen increased attention to the development of functional supramolecular architectures.[1–10] Whilst research into supramolecular chemistry continues to focus on understanding and using non-covalent forces to construct multi-component assemblies, significant effort is now directed on applying this fundamental knowledge to develop molecular assemblies that can perform tasks analogous to the machines of everyday life.[5,11–14] Examples include the cation-crown ether complexes developed into highly sensitive and selective fluoro-ionophores and simple viologen donor-acceptor interactions employed for switchable rotaxanes and catenanes.[15–18] The number of publications in the area of functional rotaxane and catenane structures has risen dramatically since the early reports on synthesis by metal–ligand coordination and statistical threading.[19–21] The functionality of hydrogen-bonding catenanes and rotaxanes has been explored with particular emphasis on the study of the relative motion of the components, that is in the synthesis and study of a molecular muscle where an interlocked rotaxane can be contracted or extended by changing the metal cation.[22,23] Leigh *et al.* have shown that photoinduced electron transfer to a naphthalimide unit alters the hydrogen-bond acceptor ability of the carbonyl groups.[24] Stoddart and co-workers have reported a series of rotaxanes and catenanes that demonstrate a diverse array of properties, such as photochemically driven molecular switches, redox switchable catenanes and slow shuttling rotaxanes.[18,25–47] Analogous neutral donor-acceptor interactions have been used in our work: the acceptor units are electron-deficient aromatic diimide units, such as pyromellitic or naphthalene diimide, and a range of symmetric and asymmetric donor-acceptor catenanes have been synthesised using either reversible alkene metathesis or irreversible Glaser coupling of terminal acetylenes.[48–52] In general additional non-covalent interactions (C–H···O bonding in particular) are required to assemble the donor and acceptor components.[52]

We have recently described a switching experiment between naphthalene diimide and pyromellitic diimide pseudorotaxanes induced by lithium cations and have incorporated this switch into a neutral rotaxane.[53,54] In an attempt to understand and generalise this cation-induced effect we have now carried out a detailed structural and kinetic study of the formation of pseudorotaxanes from donor (crown ether **1**) and acceptor (**2**) units (Fig. 1), in the presence or absence of a series of alkali salts MX such as LiBr, LiI, $Li(CF_3SO_3)$, $Li[B(C_6F_5)_4]$, NaBr, NaI, $Na(CF_3SO_3)$ and $Na[B\{3,5\text{-}(CF_3)_2(C_6H_3)\}_4]$. Solid-state structures of new pseudorotaxanes (determined by X-ray diffraction) and solution structures [determined by NMR in $CD_2Cl_2$ or a mixture of $CHCl_3$ and MeOH (98 : 2)] are discussed.

## Results and discussion

We were surprised by the way alkali metal ions affected the association of host **1** and guest **2**. When we first added alkali metal salts to solutions of **1** and **2** we intended to use the well-established interaction between crown ethers and alkali metal cations to *dissociate* the $\mathbf{1} \cdot \mathbf{2}$ pseudorotaxane complex. As it turned out, the envisaged cation-crown interaction did occur but had exactly the opposite effect to that expected: the cation *reinforced* the complexation between **1** and **2**. Evidence for this unexpected behaviour comes from visual inspection of the solutions and UV-Vis analysis. Whereas a 10.0 mM solution of guest **2** is essentially colourless, addition of 5.0 mM of the colourless host **1** gives rise to a faint yellow colour resulting from relatively inefficient complexation and charge transfer between **1** and **2**. Subsequent addition of excess alkali salt had a dramatic effect, giving coloured solutions ranging from orange to dark-red, depending on the salt. The UV-Vis spectrum in Fig. 2 shows the appearance of a charge transfer band at 468 nm upon addition of LiI, suggesting that the donor and acceptor systems are able to interact much more efficiently in the presence of LiI. The variation of $\lambda_{max}$ in lithium complexes ranges from 432 nm (LiBr) to 468 nm (LiI). In Na complexes $\lambda_{max}$ ranges from 430 nm to 482 nm ($NaB[\{3,5\text{-}(CF_3)_2(C_6H_3)\}_4]$) (Table 1). These intriguing observations prompted us to investigate the effect of a series of alkali-metal salts on the formation of $\mathbf{1} \cdot \mathbf{2}$ pseudorotaxanes in solution [in $CH_2Cl_2$ or a mixture of $CHCl_3$ and MeOH (98 : 2], using NMR

DOI: 10.1039/b415418e

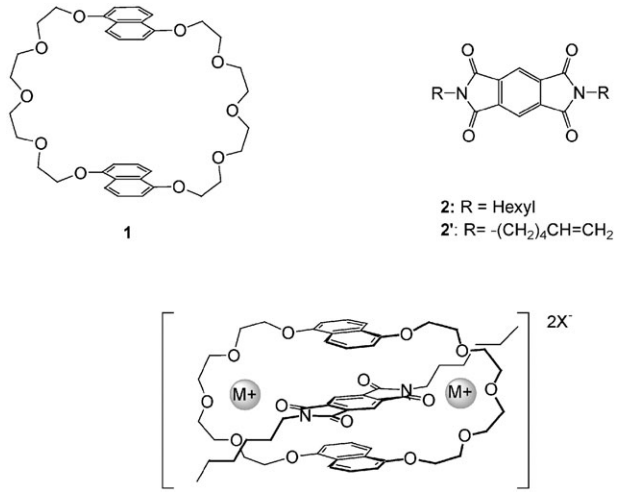


**Fig. 1** Representations of the donor host **1** and acceptor guest **2**, templates and the pseudorotaxane assembly.

and ITC, and in the solid state by single crystal X-ray diffraction. Crystal structures of the resulting complexes revealed that the Li and Na salts insert into two different remarkably well pre-organised binding sites.

### Pseudorotaxane structures in solution: NMR studies

We observed that after addition of 1 equiv. of LiI, 50% of the organic material remains unchanged, while 50% is present in a new species in slow exchange on the chemical shift timescale. Integration confirmed unambiguously the M : **1** : **2** stoichiometry of 2 : 1 : 1, implying a dramatic cooperativity between binding of the first and second cations. The same is true for all LiX investigated. The $^1$H NMR spectra allowed the elucidation of the structure of the donor-acceptor complexes of MX, where for $M^+ = Li^+$, $X^- = I^-$, $Br^-$, $CF_3SO_3^-$, $[B(C_6F_5)_4]^-$ and for $M^+ = Na^+$, $X^- = I^-$, $CF_3SO_3^-$, $[B\{3,5\text{-}(CF_3)_2(C_6H_3)\}_4]^-$. For $M^+ = Li^+$ or $Na^+$, the $^1$H NMR spectrum of the 2 : 1 : 1 complexes $[M_2 \cdot \mathbf{1} \cdot \mathbf{2}]X_2$ show a remarkable degree of symmetry. Based on the number of signals observed and discussed below, we believe that the new species exhibit in solution the general structure shown in Fig. 1.

The NMR evidence includes ring-current induced shift in the aromatic protons of guest **2**, ring-current induced shift in the naphthyl protons of the crown ether **1**, shifts in tetraethylene glycol signals and determination of effective symmetry. While the aromatic protons of the unbound pyromellitic diimide (**2**) in the presence of **1** resonate at $\delta$ 8.19 in $CD_2Cl_2$ at 280 K, this resonance shifts to 6.55 ppm upon addition of 10 equiv. of LiI, indicating that they are held in close proximity to the shielding region of the naphthyl rings. Separate peaks are observed for bound and unbound guest **2**, indicating that dissociation of **2** is slow on the NMR chemical shift timescale. Similar shifts were observed for a range of alkali salts (Table 2).

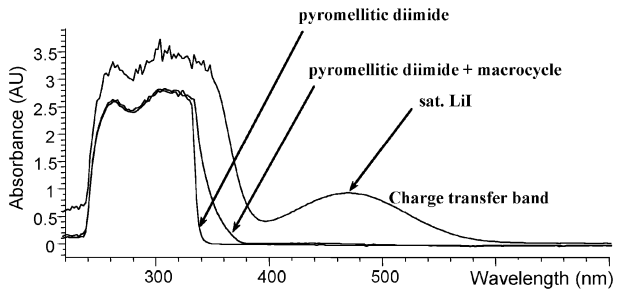


**Fig. 2** UV-Vis spectra of the indicated species (5.0 mM) taken in $CH_2Cl_2$ solution.

**Table 1** UV-Vis data for a series of pseudorotaxanes (5.0 mM solution in $CD_2Cl_2$)

| MX | $\lambda_{max}$/nm | $\Delta E$/eV | $E_{max}$/L mol$^{-1}$ cm$^{-1}$ |
|---|---|---|---|
| LiBr | 432 | 2.87 | 187.8 |
| LiI | 468 | 2.65 | 610.6 |
| $Li(CF_3SO_3)$ | 466 | 2.66 | 453.0 |
| $LiB(C_6F_5)_4$ | 462 | 2.68 | — |
| NaBr | 430 | 2.88 | 151.2 |
| NaI | 452 | 2.77 | 763.6 |
| $Na(CF_3SO_3)$ | 454 | 2.73 | 578.0 |
| $NaB[\{3,5\text{-}(CF_3)_2(C_6H_3)\}_4]$ | 482 | 2.65 | — |

The four (shifted) aromatic peaks are not split, showing that the high degree of symmetry is retained when the alkali metal is incorporated into the complex. The large upfield shifts of the signals of the naphthalene proton ($H_1$, $H_2$, $H_3$ labelled as in Fig. 3) confirm the presence of the pyromellitic diimide guest in a sandwich structure, as in our related catenane structure.[52] Chemical shifts of the aromatic proton $H_4$ of the bound guest differ in LiI *vs.* NaI complexes by *ca.* 1 ppm (in $CD_2Cl_2$ at 200 K, Fig. 4 and Table 2). Almost identical chemical shifts for the *aromatic* bound crown ether resonances $H_1$–$H_3$ were observed regardless of the nature of the cation. For all complexes, COSY experiments confirm the expected proton couplings of the naphthalene rings. The free macrocycles contain four distinct carbon environments for the tetraethylene glycol moiety. The number of different environments does not change in the $[M_2 \cdot \mathbf{1} \cdot \mathbf{2}]^{2+}$ complex (according to the $^{13}$C NMR spectrum), consistent with the retention of the high degree of symmetry after complexation. Binding of two lithium cations results in the geminal splitting of the tetraethylene glycol protons, as indicated by HMQC. The proposed structure $[M_2 \cdot \mathbf{1} \cdot \mathbf{2}]X_2$ (Fig. 1) satisfies all steric, electrostatic, charge transfer and symmetry requirements for all complexes. Since no significant binding was observed by NMR for NaBr, further investigations were not performed. A lower ion-pair dissociation constant for NaBr combined with low solubility in $CH_2Cl_2$ probably explains its lack of complexation.[55]

A closer inspection of chemical shift differences in the series suggested that use of sodium instead of lithium salts, combined with differing size of the anions, results in subtly different geometries of the resulting complexes. The orientation of the guest with respect to the host (Table 1, Fig. 3) was derived from variable temperature 1D and 2D NOESY experiments in $CD_2Cl_2$. Fig. 3 shows the labelling for free and bound host and guest molecules. The donor-acceptor arrangement varies in the series from parallel (with varying degrees of distortion from the ideal geometry) to perpendicular and will be discussed below.

**Table 2** Spectroscopic data for bis-cationic pseudorotaxanes (ppm, $CD_2Cl_2$, for labelling see Fig. 3)

| MX | $T$/K | $H_1$ | $H_2$ | $H_3$ | $H_4$ | $H_6$[a] |
|---|---|---|---|---|---|---|
| None | 280 | 7.70 | 7.17 | 6.48 | 8.19 | 4.04 |
| LiI | 280 | 6.98 | 6.81 | 6.58 | 6.55 | 5.06 |
| LiI | 200 | 6.90 | 6.77 | 6.54 | 6.18 | 4.66 |
| LiBr | 280 | 6.98 | 6.78 | 6.56 | 6.75 | 5.17 |
| $Li(CF_3SO_3)$ | 280 | 6.98 | 6.80 | 6.52 | 6.43 | 4.50 |
| $LiB(C_6F_5)_4$[b] | 280 | 7.07 | 6.84 | 6.48 | 6.64 | 3.64 |
| NaI | 200 | 6.88 | 6.75 | 6.54 | 7.13 | 5.28 |
| $Na(CF_3SO_3)$ | 240 | 7.06 | 6.81 | 6.36 | 6.76 | — |
| $NaB[\{3,5\text{-}(CF_3)_2(C_6H_3)\}_4]$[c] | 280 | 7.17 | 6.86 | 6.30 | 7.07 | 3.56 |

[a] $H_6$: for metal complexes only the downfield-shifted diastereotopic protons are reported. [b] $^{19}$F: $\delta$ − 131.6 (br, ortho-F), −161.8 (td, $^3J_{FF}$ = 18.8 Hz, meta-F), −165.8 (td, $^3J_{FF}$ = 18.8 Hz, para-F); $^{11}$B{$^1$H}: $\delta$ − 3.7; $^7$Li: $\delta$ 0.02. [c] $^{19}$F: $\delta$ − 63.65; $^{11}$B{$^1$H}: $\delta$ − 3.79.

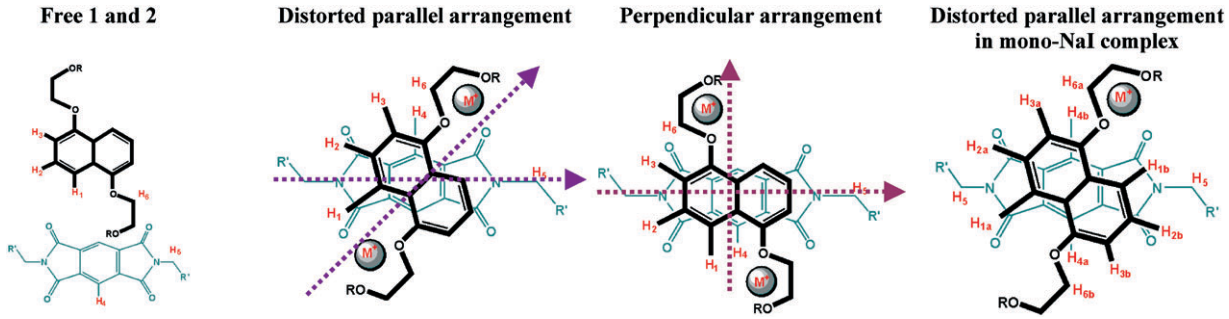


**Fig. 3** Schematic drawing of main geometry arrangements for pseudorotaxane complexes.



For all lithium complexes, the guest aromatic protons $H_4$ show NOEs with the naphthalene rings protons $H_1$–$H_3$, as well as with the tetraethylene glycol protons. $H_3$ also shows NOEs to glycol loops $OCH_2CH_2$ and $H_4$ shows NOE to the most downfield shifted $OCH_2CH_2$ proton $H_6$. In addition, the NOESY spectrum reveals NOEs between the aromatic protons of the naphthalene rings and the alkyl chains of the pyromellitic diimide as follows: $H_1$ shows NOEs to $NCH_2CH_2$ > $NCH_2$ > $N(CH_2)_2CH_2$, $H_2$ 'sees' $NCH_2CH_2$ > $N(CH_2)_2CH_2$. These results suggest a distorted parallel host–guest arrangement in solution for all lithium-containing pseudorotaxanes.

No satisfactory NOE results were obtained for the Na complexes due to a combination of precipitation and low intensities. The study of the NaI complex was complicated by the formation of a mono-NaI complex, in *ca.* 36% yield as estimated by integration. Since the bis-NaI complex showed similar chemical shifts for the proton resonances of the bound crown (at 200 K in $CH_2Cl_2$) to those found for the bis-LiI complex, a distorted parallel host–guest arrangement is proposed (Table 1 and Fig. 3).

At 200 K and in $CD_2Cl_2$ or $CD_3OD$ : MeOD 98 : 2 solutions, a slow exchange was observed between the bis-NaI complex and the mono-NaI complex.[56] Saturation transfer experiments show that this exchange takes place *stepwise*: free guest **2** is in exchange with the mono-NaI complex and the mono-NaI complex is in exchange with the free crown ether **1** as well as the bis-NaI pseudorotaxane. This behaviour was not observed (on the NMR timescale and above 200 K) for the complexes of $Na(CF_3SO_3)$ or $Na[B\{3,5\text{-}(CF_3)_2(C_6H_3)\}_4]$. Interestingly, the diagnostic resonances ($H_4$) for the guest molecule in the mono-NaI complex were found at $\delta$ 5.75 and 7.75, consistent with the lower symmetry of the system caused by shielding from only one side of the molecule (Table 3). Assignments of the mono-NaI complex were aided by a COSY spectrum. Correlations were observed between $H_1$a and $H_1$b, $H_4$a and $H_4$b, $H_1$a, $H_2$a and $H_3$a, $H_1$b, $H_2$b and $H_3$b. There is little exchange between the asymmetric sides of both the crown and the pyromellitic diimide, but $H_1$a and $H_1$b can be 'linked' *via* the bis-NaI complex $H_1$. Similarly $H_2$a and $H_2$b are 'linked' *via* $H_2$ of the bis-NaI complex and $H_3$a and $H_3$b are linked *via* $H_3$ of the bis-NaI complex. The structure of the mono-NaI complex has not yet been determined in the solid state and exchange with the bis-NaI complex in solution made uncertain the assignment of the relative donor-acceptor orientation by NMR. Since no formation of mono-MX complexes was detected in any other cases, cooperative binding of the cation is occurring. The absence of a 1 : 1 : 1 complex is significant with respect to the mechanism of formation of the $[Li_2 \cdot \mathbf{1} \cdot \mathbf{2}]^{2+}$ complex. The stability of the 2 : 1 : 1 complex $[Li_2 \cdot \mathbf{1} \cdot \mathbf{2}]^{2+}$ is clearly orders of magnitude higher than that of $[Li \cdot \mathbf{1} \cdot \mathbf{2}]^{2+}$.

It appears that the choice of cation is limited by the size of the binding cavity, since attempted template reactions with K, Rb and Cs ions had no effect on the neutral donor-acceptor complex. However, the low solubility of these salts in $CH_2Cl_2$ may also explain this observation.

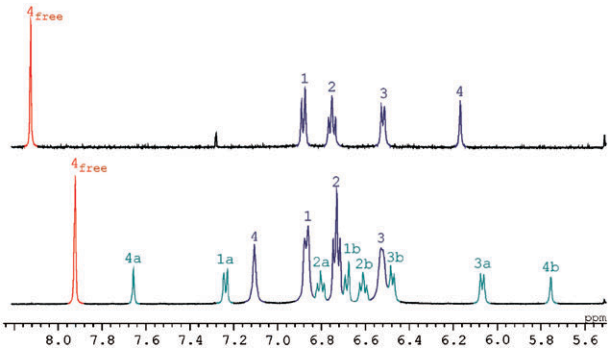


**Fig. 4** $^1$H NMR spectrum of (a) LiI and (b) mono-NaI and bis-NaI complexes.

## Solid-state pseudorotaxane structures

A search of the Cambridge Structural Database revealed that only 16 supramolecular complexes using the donor crown ether **1** as the host have been reported so far,[30,52,57–67] in addition to the structure of the free **1**.[30] Amongst these, only two are derivatives of the guest **2** and they are both catenanes.[52,66] Crystallisation of single crystals from either $CH_2Cl_2$ (complexes $[Li_2 \cdot \mathbf{1} \cdot \mathbf{2}][B(C_6F_5)_4]_2$ and $[Na_2 \cdot \mathbf{1} \cdot \mathbf{2}][B\{3,5\text{-}(CF_3)_2(C_6H_3)\}_4]_2$) or a mixture of $CHCl_3$ : MeOH 98 : 2 was successful {complexes $[Li_2 \cdot \mathbf{1} \cdot \mathbf{2}']I_2$,[53] $[Li_2 \cdot \mathbf{1} \cdot \mathbf{2}]Br_2$, $[Li_2 \cdot \mathbf{1}]I_2$ and $[Na_2 \cdot \mathbf{1} \cdot \mathbf{2}]I_2$} and the solid-phase structures of these complexes have been determined by X-ray crystallography (Figs. 5–10, Tables 4 and 5).

The two related geometries found in solution, distorted parallel and perpendicular, are retained in the solid state. Host–guest torsion angles (defined as in Fig. 3) are around 40° for the Li complexes, 57° for NaI and almost 90° for $NaB[\{3,5\text{-}(CF_3)_2(C_6H_3)\}_4]$. The distortion from the ideal geometry accompanies the increase in the bulkiness of the anion. For Li complexes, the variation in host–guest torsion angle is not large (up to *ca.* 3.4°), whereas the corresponding difference between

**Table 3** Spectroscopic data for the mono-NaI pseudorotaxane (NMR assignments assisted by 1D-NOESY, $CD_2Cl_2$)

| NMR shift $\delta$ | Assignment |
|---|---|
| 7.26 | $H_{1a}$ |
| 6.82 | $H_{2a}$ |
| 6.08 | $H_{3a}$ |
| 7.69 | $H_{4a}$ |
| 4.75 | $H_{6a}$ |
| 6.70 | $H_{1b}$ |
| 6.62 | $H_{2b}$ |
| 6.49 | $H_{3b}$ |
| 5.76 | $H_{4b}$ |
| 4.17 | $H_{6b}$ |

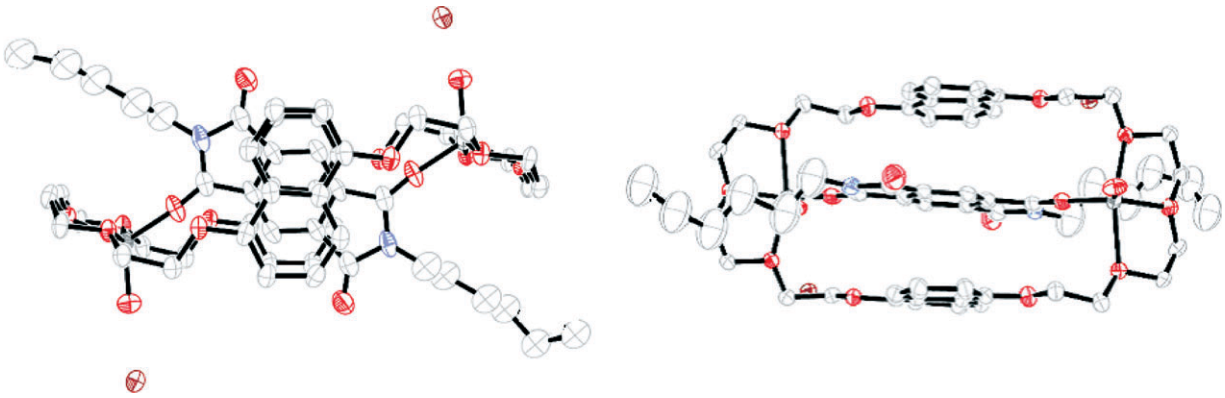

**Fig. 5** Two views (ORTEP plot at 30% probability) of the X-ray molecular structure of complex $[Li_2 \cdot \mathbf{1} \cdot \mathbf{2}]Br_2$. Hydrogens are omitted for clarity. (Br: brown, N: light blue, Li: dark grey, O: red, C: light grey)



$[Na_2 \cdot \mathbf{1} \cdot \mathbf{2}][B\{3,5\text{-}(CF_3)_2(C_6H_3)\}_4]_2$ and $[Na_2 \cdot \mathbf{1} \cdot \mathbf{2}]I_2$ is larger than 30°.

In the complex $[Na_2 \cdot \mathbf{1} \cdot \mathbf{2}]I_2$, NaI remains associated (Na–I separation *ca.* 3.03 Å) with the sodium centre in a distorted trigonal bipyramidal geometry rendering a distorted parallel donor-acceptor arrangement. In $[Na_2 \cdot \mathbf{1} \cdot \mathbf{2}][B\{3,5\text{-}(CF_3)_2(C_6H_3)\}_4]_2$, coordination of counter-ions to $Na^+$ occurs through the $CF_3$ groups of the bulky anion. As expected, each of the $CF_3$ groups of $[B\{3,5\text{-}(CF_3)_2(C_6H_3)\}_4]^-$ is disordered over two positions and a difference electron density map showed six clear positions for the fluorine atoms in each of the $CF_3$ groups, with almost equal peak size. It was possible to observe that two fluorine atoms on the same $CF_3$ group occupy the 5th and 6th coordination sites of the sodium centre (the two Na–F separations are 2.45 and 2.87 Å). The geometry of the Na atoms is therefore octahedral (but greatly distorted), in which two of the equatorial sites are occupied by two of the fluorine atoms belonging to one of the $CF_3$ groups of $B[3,5\text{-}(CF_3)_2(C_6H_3)]_4^-$.

The lithium cations are all five-coordinate with a greatly distorted coordination geometry that most closely resembles a trigonal bipyramidal arrangement. The fifth coordination site is filled by an additional donor molecule, for example a water molecule for $[Li_2 \cdot \mathbf{1} \cdot \mathbf{2}']I_2$, $[Li_2 \cdot \mathbf{1} \cdot \mathbf{2}]Br_2$, $[Li_2 \cdot \mathbf{1} \cdot \mathbf{2}][B(C_6F_5)_4]_2$ and $[Li_2 \cdot \mathbf{1}]I_2$. For $[Li_2 \cdot \mathbf{1} \cdot \mathbf{2}']I_2$[53] and $[Li_2 \cdot \mathbf{1} \cdot \mathbf{2}]Br_2$ the preference for water over methanol to fill the fifth coordination site is remarkable considering the large excess of methanol in solutions of $[Li_2 \cdot \mathbf{1}]I_2$, $[Li_2 \cdot \mathbf{1} \cdot \mathbf{2}']I_2$ and $[Li_2 \cdot \mathbf{1} \cdot \mathbf{2}]Br_2$ (2% solution ≡ 90 equiv. of methanol). In the case of $[Li_2 \cdot \mathbf{1}]I_2$, in the absence of a guest, this site is occupied by one molecule of methanol for each of the lithium atoms, therefore maintaining the five-coordinate geometry.

Intermolecular stacking between pseudorotaxane units in the unit cell has not been observed for any of the complexes. For the lithium halide complexes, the anion is not directly coordinated to the complex and no ion-pairing was observed. This observation is also consistent with NMR experiments that suggested that the solution structures of the lithium complexes are not significantly influenced by the nature of the anion when $X^- = I^-$ or $Br^-$. Our observations are consistent with those by Huang *et al.* regarding the direct correlation between ion-pairing in solid state and in solution.[55]

By contrast, for complexes $[Li_2 \cdot \mathbf{1} \cdot \mathbf{2}][B(C_6F_5)_4]_2$ and $[Na_2 \cdot \mathbf{1} \cdot \mathbf{2}][B\{3,5\text{-}(CF_3)_2(C_6H_3)\}_4]_2$ the large counter-ion is involved in a series of intermolecular hydrogen bonds, which in the case of $[Li_2 \cdot \mathbf{1} \cdot \mathbf{2}][B(C_6F_5)_4]_2$ give rise to a supramolecular array. In the 3D network of $[Li_2 \cdot \mathbf{1} \cdot \mathbf{2}][B(C_6F_5)_4]_2$ hydrogen bonds link pseudorotaxane units and the counter-ions: the lithium-coordinated molecule of water is strongly hydrogen-bonded to F(6) from a neighbouring $[B(C_6F_5)_4]^-$ unit (and the same is true for the symmetry-generated pair). The separation O(8)–F(6A) [where F(6A) belongs to the asymmetric unit generated by the symmetry operator $x$, $y$, $1 + z$] is 2.983(1) Å. Furthermore, the acceptor molecule within the pseudorotaxane shows intermolecular hydrogen bonds between the $N(CH_2)$ units and the fluorine atoms of adjacent counter-ions. These interactions are directed perpendicular with respect to the acceptor's plane (below and above this plane) with a separation between C(6) and F(13A) of 2.991(1) Å (where the latter atom belongs to the asymmetric unit generated by the symmetry operator $x$, $1 + y$, $z$). In addition, it appears that all fluorine atoms of $[B(C_6F_5)_4]^-$ are within short distances to neighbouring hydrogen of the glycol chain of the crown ether, with C(glycol)–F separations ranging between 2.9 and 3.7 Å. These short distances seem to

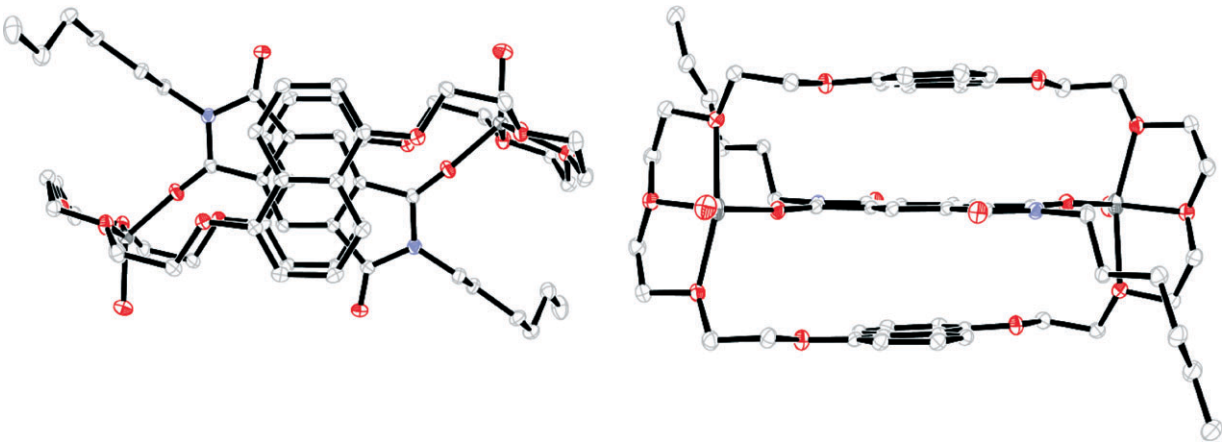

**Fig. 6** Two views (ORTEP plot at 30% probability) of the X-ray molecular structure of $[Li_2 \cdot \mathbf{1} \cdot \mathbf{2}][B(C_6F_5)_4]_2$. Counter-ions and hydrogen atoms are omitted for clarity. (N: light blue, Li: dark grey, O: red, C: light grey)

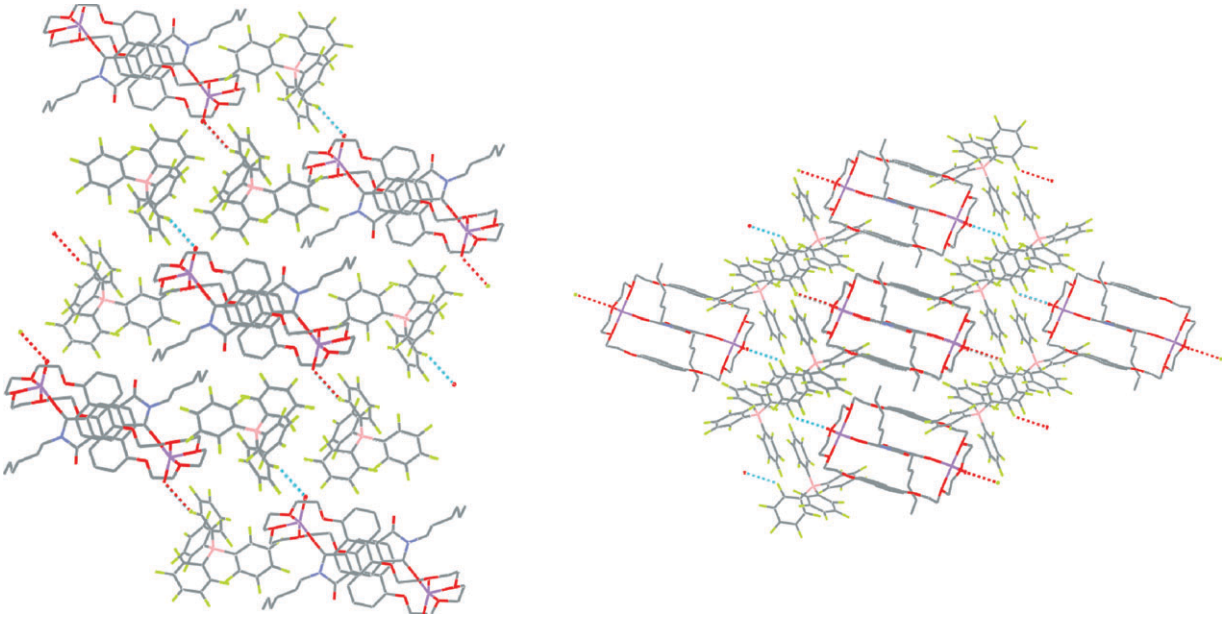

**Fig. 7** Packing diagram of the $[Li_2 \cdot \mathbf{1} \cdot \mathbf{2}][B(C_6F_5)_4]_2$ complex, views over the *a* and *c* axes, respectively. (B: pink, F: green, N: light blue, Li: dark grey, O: red, C: light grey)



be maintained in $CD_2Cl_2$ solutions, since $^1H$ NMR showed reduced chemical shift differences between the diastereotopic O–$CH_2$ (glycol) chain in $[Li_2 \cdot \mathbf{1} \cdot \mathbf{2}][B(C_6F_5)_4]_2$ ($\Delta\delta$ = 0.1) with respect to those found in the LiI or LiBr ($\Delta\delta$ *ca.* 1.2) and $Li(CF_3SO_3)$ complexes ($\Delta\delta$ *ca.* 0.5).

The Na–Na distance in $[Na_2 \cdot \mathbf{1} \cdot \mathbf{2}][B\{3,5\text{-}(CF_3)_2(C_6H_3)\}_4]_2$ is 10.63 Å, similar to the 10.08 Å measured for $[Na_2 \cdot \mathbf{1} \cdot \mathbf{2}]I_2$. The Li–Li distance does not vary significantly in the series, being 11.02 Å in $[Li_2 \cdot \mathbf{1} \cdot \mathbf{2'}]I_2$, 10.8 Å in $[Li_2 \cdot \mathbf{1} \cdot \mathbf{2}]B(C_6F_5)_4]_2$ and 10.89 Å in $[Li_2 \cdot \mathbf{1}]I_2$. In general, the inter-planar separations between the host and guest rings in the series range from 3.27 to 3.48 Å with higher values for sodium complexes. The cavity size of the guest-free complex $[Li_2 \cdot \mathbf{1}]I_2$ is 6.42 Å, that is the mid-distance between naphthyl groups of the crown ether is 3.21 Å. The two donor units are essentially coplanar with a deviation smaller than 0.5°. These values are consistent with the inter-planar separations of published catenanes[52,66,67] and confirm the donor-acceptor interaction between the host and the guest, as well as the pre-organised nature of the host. The crystal structures indicate that the size of the cation that can be accommodated is limited by the size of the binding cavity (Fig. 11).

### NMR studies on the kinetic stability of complexes

In an attempt to estimate the influence of different MX salts on the kinetic stability of the pseudorotaxanes $[M_2 \cdot \mathbf{1} \cdot \mathbf{2}]X_2$, we studied the rate constants for complex dissociation in $CD_2Cl_2$ solution ($k_{-1}$) using 1D NOESY NMR experiments.[68–71] Complexes were obtained using a twofold excess of guest **2**

**Fig. 8** Two views (ORTEP plot at 30% probability) of the X-ray molecular structure of $[Li_2 \cdot \mathbf{1}]I_2$. Hydrogens are omitted for clarity. (N: light blue, Li: dark grey, O: red, C: light grey, I: purple)

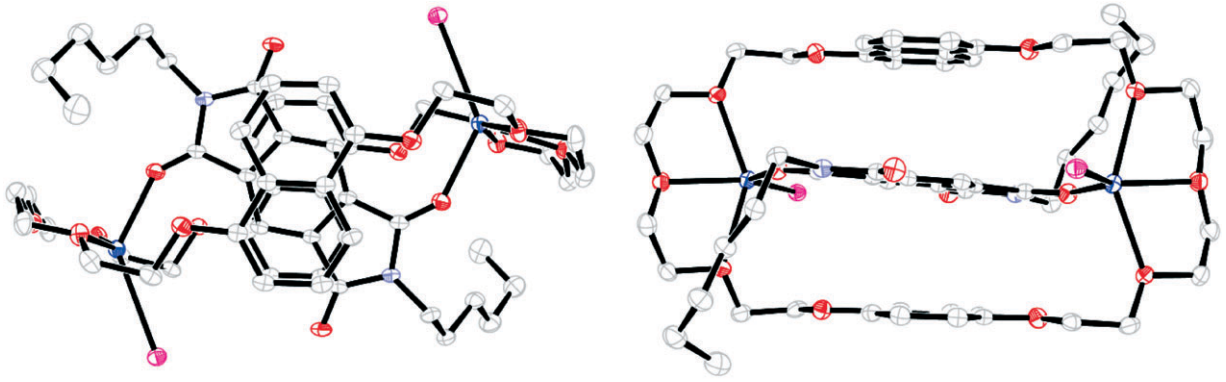

**Fig. 9** Two views (ORTEP plot at 30% probability) of the X-ray molecular structure of $[Na_2 \cdot \mathbf{1} \cdot \mathbf{2}]I_2$. Hydrogens are omitted for clarity. (N: light blue, Li: dark grey, O: red, C: light grey, I: purple, Na: dark blue)

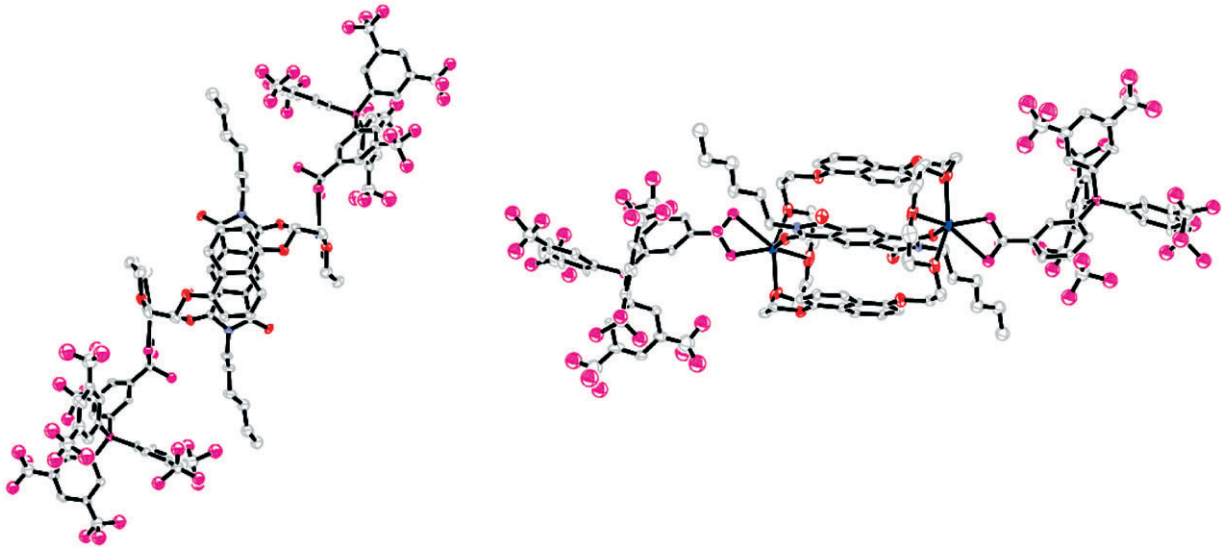

**Fig. 10** Two views (ORTEP plot at 30% probability) of the X-ray molecular structure of $[Na_2 \cdot \mathbf{1} \cdot \mathbf{2}][B\{3,5\text{-}(CF_3)_2(C_6H_3)\}_4]$. Hydrogens are omitted for clarity. (N: light blue, Li: dark grey, O: red, C: light grey, I: purple, Na: dark blue)



**Table 4** Relevant molecular parameters (from X-ray diffraction studies) for selected complexes

| Compound | $[Li_2 \cdot \mathbf{1} \cdot \mathbf{2}']I_2$[a] | $[Li_2 \cdot \mathbf{1} \cdot \mathbf{2}]Br_2$ | $[Li_2 \cdot \mathbf{1} \cdot \mathbf{2}]B[(C_6F_5)_4]_2$ | $[Li_2 \cdot \mathbf{1}]I_2$ | $[Na_2 \cdot \mathbf{1}]I_2$ | $[Na_2 \cdot \mathbf{1} \cdot \mathbf{2}][B\{3,5\text{-}(CF_3)_2(C_6H_3)\}]_4$ |
|---|---|---|---|---|---|---|
| M–O ($A_1$)/Å | 1.8783 (*x*) | 1.8874 | 1.89 | — | 2.2716 | 2.33 |
| M–O ($D_1$)/Å | 2.2488 (*x*) | 2.2401 | 2.3 | 2.1425 | 2.4871 | 2.35 |
| | 1.9668 (*x*) | 1.954 | 1.97 | 1.978 | 2.3181 | 2.34 |
| | 2.2903 (*x*) | 2.234 | 2.19 | 2.5513 | 2.4226 | 2.35 |
| M–Ligand/Å | 1.8823 (*y*)[b] | 1.9251[b] | 1.95[b] | 1.9096[b] | 3.0308[c] | 2.93[d] |
| | — | — | — | 1.9246[e] | — | — |
| M–M/Å | 11.02 | 11.06 | 10.83 | 10.89 | 10.08 | 10.63 |
| $D_1$–$A_1$/Å | 3.27 | 3.28 | 3.34 | —[f] | 3.41 | 3.48 |
| Torsion angle $D_1$–$A_1$/° | 38.3 | 37.1 | 41.5 | — | 57.6 | 89.05 |

[a] Ref. 53. [b] Ligand = $H_2O$. [c] Ligand = I. [d] Ligands = two fluorines (disordered $CF_3$). [e] Ligand = MeOH. [f] 2 × (distance $D_1$–$D_1$) = 6.42 Å.

**Table 5** Selected crystallographic data for studied complexes

| Compound | $[Li_2 \cdot \mathbf{1} \cdot \mathbf{2}]Br_2 \cdot 5CH_2Cl_2 \cdot 2H_2O$ | $[Li_2 \cdot \mathbf{1} \cdot \mathbf{2}][B(C_6F_5)_4]_2 \cdot 2CH_2Cl_2 \cdot 2H_2O$ | $[Li_2 \cdot 1]I_2 \cdot 2MeOH \cdot 2H_2O$ | $[Na_2 \cdot \mathbf{1} \cdot \mathbf{2}]I_2 \cdot 6CH_2Cl$ | $[Na_2 \cdot \mathbf{1} \cdot \mathbf{2}][B\{3,5\text{-}(CF_3)_2(C_6H_3)\}_4]_2$ |
|---|---|---|---|---|---|
| Formula | $C_{63}H_{81}Br_2Cl_{15}N_2O_{16}$ | $C_{108}H_{76}B_2Cl_4F_{40}Li_2N_2O_{16}$ | $C_{38}H_{56}I_2Li_2O_{14}$ | $C_{64}H_{78}Cl_{18}I_2N_2Na_2O_{14}$ | $C_{122}H_{96}B_2F_{48}N_2Na_2O_{14}$ |
| *M* | 1827.73 | 2595.03 | 1004.55 | 2037.16 | 2793.36 |
| $\lambda$/Å | 0.71073 | 0.71073 | 0.6923[a] | 0.71073 | 0.71073 |
| *T*/K | 180 (2) | 180 (2) | 150 (2) | 180 (2) | 180 (2) |
| Crystal system | Monoclinic | Triclinic | Triclinic | Triclinic | Monoclinic |
| Space group | $P2_1/c$ | $P$ -1 | $P$ -1 | $P$ -1 | $C2/c$ |
| *a*/Å | 15.8820(3) | 10.7147(2) | 7.566(1) | 10.8071(2) | 38.5110(1) |
| *b*/Å | 10.2424(2) | 13.4449(2) | 10.3074(14) | 11.2503(2) | 15.7246(2) |
| *c*/Å | 26.2432(6) | 19.5512(3) | 15.598(2) | 18.3062(3) | 22.8791(3) |
| $\alpha$/° | | 103.2331(7) | 72.355(2) | 78.4706(8) | |
| $\beta$/° | 94.5550(7) | 90.1735(7) | 88.102(2) | 81.8524(7) | 93.6400(5) |
| $\gamma$/° | | 94.5532(7) | 81.429(2) | 86.3758(12) | |
| *U*/Å$^3$ | 4255.49(15) | 2732.42(8) | 1146.2(3) | 2157.41(7) | 13826.9(3) |
| *Z* | 2 | 1 | 1 | 1 | 4 |
| $\rho_{calc}$/g cm$^{-3}$ | 1.426 | 1.577 | 1.455 | 1.568 | 1.342 |
| $\mu$/mm$^{-1}$ | 1.481 | 0.243 | 1.430 | 1.352 | 0.135 |
| Total data | 24872 | 20750 | 8794 | 21614 | 87214 |
| Unique data | 7714 | 12240 | 6117 | 9407 | 15601 |
| $R_{int}$ | 0.057 | 0.045 | 0.03 | 0.033 | 0.078 |
| $R$ [$I > 3\sigma(I)$] | 0.1000 | 0.0452 | 0.0342 | 0.0344 | 0.1580 |
| *wR* | 0.1184 | 0.0562 | 0.0367 | 0.0444 | 0.1728 |

[a] Synchrotron radiation, Station 9.8, Daresbury SRS.

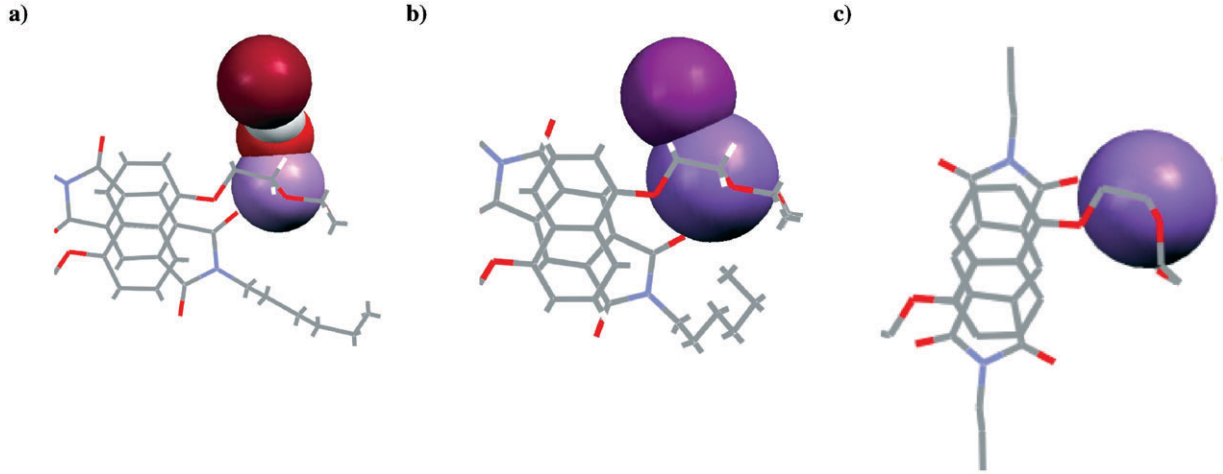


**Fig. 11** Binding of cations inside the pseudorotaxane cavity: (a) $[Li_2 \cdot \mathbf{1} \cdot \mathbf{2}]Br_2$, (b) $[Na_2 \cdot \mathbf{1} \cdot \mathbf{2}]I_2$, (c) $[Na_2 \cdot \mathbf{1} \cdot \mathbf{2}][B\{3,5\text{-}(CF_3)_2(C_6H_3)\}_4]$.



and a tenfold excess of the MX salt. The 1D NOESY experiments showed that the free and bound guest **2** species are in exchange, for each of the different MX salts.

The temperature for each experiment was chosen such that the exchange process was slow on the NMR chemical shift timescale. The chemical shifts of the exchanging resonances were not significantly temperature dependent. For each complex, the resonances corresponding to the methyl and the $H_4$ protons of the bound guest **2** were irradiated in turn and the responses of the corresponding resonances of the free guest were measured. The rates of complex dissociation were then extracted using the initial rate approximation method.[69–71]

For $[Li_2 \cdot \mathbf{1} \cdot \mathbf{2}]I_2$, rate constants $k_{-1}$ in $CD_2Cl_2$ were obtained for temperatures ranging from 290 to 315 K and the activation parameters for complex dissociation were determined from an Eyring plot (Fig. 12).[72]

We use relative rates to illustrate the kinetic stability differences in the $[M_2 \cdot \mathbf{1} \cdot \mathbf{2}]X_2$ series: the relative rates were obtained by extrapolating each $k_{-1}$ to 315 K while setting the slowest exchange at 315 K {for the $[Li_2 \cdot \mathbf{1} \cdot \mathbf{2}]I_2$ complex in $CD_2Cl_2$} to unity (Table 6). This assumes that the free energy of activation does not change within that temperature range. Note that the equilibrium constants $K$ could not be calculated, due to the absence of free host **1** from the system.

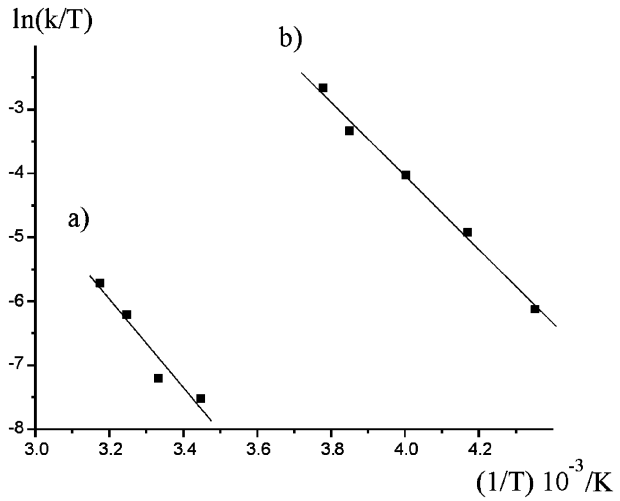


**Fig. 12** Estimation of dissociation barrier for the LiI complex by Eyring plot [Eyring plot: $\ln(k/T) = -\Delta H^{\#}/RT + \Delta S^{\#}/R + 23.76$; estimated uncertainty on $k$ ±20%]. (a) In $CD_2Cl_2$: $\Delta H^{\#} = 54.6$ kJ mol$^{-1}$, $\Delta S^{\#} = -72.0 \times 10^{-3}$ kJ mol$^{-1}$ K$^{-1}$, $\Delta G^{\#}$ (273 K) = 74.3 kJ mol$^{-1}$. (b) In a $CHCl_3$ : MeOD mixture (98 : 2): $\Delta H^{\#} = 47.9$ kJ mol$^{-1}$, $\Delta S^{\#} = -39.6 \times 10^{-3}$ kJ mol$^{-1}$ K$^{-1}$, $\Delta G^{\#}$ (273 K) = 58.7 kJ mol$^{-1}$.

A kinetically more stable complex requires a higher temperature to achieve a given rate of exchange. Thus, for the $[Li_2 \cdot \mathbf{1} \cdot \mathbf{2}]X_2$ series (in $CD_2Cl_2$) LiI forms the most kinetically stable complex, followed by LiBr, $LiB(C_6F_5)_4$ and $Li(CF_3SO_3)$ (Table 6).

The relative kinetic stabilities of the $[Na_2 \cdot \mathbf{1} \cdot \mathbf{2}]X_2$ complexes could not be determined for a variety of reasons. For example, the NaI complex shows a more complex exchange behavior, involving a fast interchange between the mono-NaI and bis-NaI complexes, as well as a much slower dissociation to the free guest **2** species. Reliable data (from 1D NOESY experiments) could only be obtained for the exchange between the two NaI complexes and not for the dissociation. Although the spectrum of $[Na_2 \cdot \mathbf{1} \cdot \mathbf{2}]X_2$ at 200 K is sharp, no dissociation is observed at this temperature: only slow exchange between the mono-NaI and bis-NaI species. At higher temperatures, at which dissociation should occur, the signals for the bound guest **2** resonances are broad: this is due to the fast exchange between the mono- and bis-NaI complexes at these temperatures.

### ITC studies on the thermodynamics of pseudorotaxane formation

We have determined the apparent association constants for binding of **1** to **2** in the presence and absence of LiI in a mixture of $CHCl_3$ : MeOH 98 : 2, using isothermal titration microcalorimetry (ITC). This technique allows direct determination of

**Table 6** Summary of activation barriers for dissociation of different pseudorotaxanes (in $CD_2Cl_2$ unless noted otherwise) obtained by 1D NOESY (EXSY) experiments at different temperature at 500 MHz. The rate constants were obtained by the initial rate approximation method. Estimated uncertainty on rate constants ±20%. Relative rates are obtained by extrapolating each $k_{-1}$ (s$^{-1}$) to 315 K while setting the slowest exchange (LiI in $CD_2Cl_2$) to unity. This assumes that the free activation energy does not change in that temperature range

| MX | $T$/K | $k_{-1}$/s$^{-1}$ | Rel. rate |
|---|---|---|---|
| LiI[a] | 315 | 1.0 | 1 |
| LiBr | 280 | 1.7 | 50 |
| $Li(CF_3SO_3)$ | 280 | 4 | 100 |
| $LiB(C_6F_5)_4$ | 280 | 3 | 80 |
| NaI | 200 | 2.0[b] | $10^6$ |
| $Na(CF_3SO_3)$ | — | — | $>10^4$ [c] |
| $NaB[\{3,5\text{-}(CF_3)_2(C_6H_3)\}_4]$ | 280 | 1.7 | 50 |

[a] Ref. 72. [b] Exchange between the mono-NaI complex and the bis-NaI complex. [c] Estimated based on broadening of resonances at different temperatures.

**Table 7** Apparent equilibrium constants and thermodynamic parameters of binding of **1** to **2** in the presence and absence of LiI

| | No LiI[a] | 10 equiv. LiI[b] |
|---|---|---|
| $K/M^{-1}$ | 21 | $2.1 \times 10^2$ |
| $\Delta G^\circ$/kJ mol$^{-1}$ | −7.6 | −13 |
| $\Delta H^\circ$/kJ mol$^{-1}$ | −7.5 | −12 |
| $T\Delta S^\circ$/kJ mol$^{-1}$ | 0.1 | 1 |

[a] A 250.0 mM solution of **1** was titrated into a 25.0 mM solution of **2**. [b] A 200 mM solution of **2** was titrated into a solution containing 50 mM LiI and 5.0 mM of **1**.

the binding constant (and, hence, $\Delta G^\circ$) and enthalpy of binding and therefore allows calculation of the entropy of binding. The results are shown in Table 7. Without any alkali metal ion the association is based solely on stacking interactions between the aromatic systems of the donor and acceptor and is relatively weak ($K$ = 21 M$^{-1}$ in a mixture of $CHCl_3$ : MeOH 98 : 2). In the presence of LiI, analysis of the binding process is complex since a termolecular complex is formed. However, we have chosen to titrate **2** into a solution of **1** containing a large excess of LiI and under these conditions it is reasonable to assume that binding of $Li^+$ to **1** is essentially complete, since this could not be independently measurable due to method limitations. Furthermore, the use of a large excess of LiI ensures that the concentration of $I^-$ counterions in the solution is relatively constant independent of the presence of the complex, thus eliminating complications arising in the determination of the dissociation constant for the ion pair.[73] Data analysis is now simplified since we only need to consider 1 : 1 binding of the acceptor to the pre-formed $[Li_2 \cdot \mathbf{1}]I_2$ complex. Fig. 13 shows the results of the titration of a 200 mM solution of acceptor into a solution containing 5.0 mM crown ether and 50 mM LiI and the fit to a 1 : 1 binding model. Also shown is the control experiment in which the acceptor solution is diluted into solvent, which shows nearly constant heat effects, indicating that the acceptor does not self-associate to any significant extent, despite the high concentration that had to be used. The results indicate that in the presence of 50 mM LiI the effective affinity for the acceptor increases 10-fold.

Inspection of the thermodynamic parameters in Table 7 indicates that, in the absence as well as in the presence of LiI, binding is completely enthalpy-driven and involves essentially no change in entropy. Apparently the loss of translational and rotational entropy of the donor and acceptor parts of the complex that has to occur upon binding is exactly compensated for by the gain in entropy caused by liberation of solvent molecules upon binding.

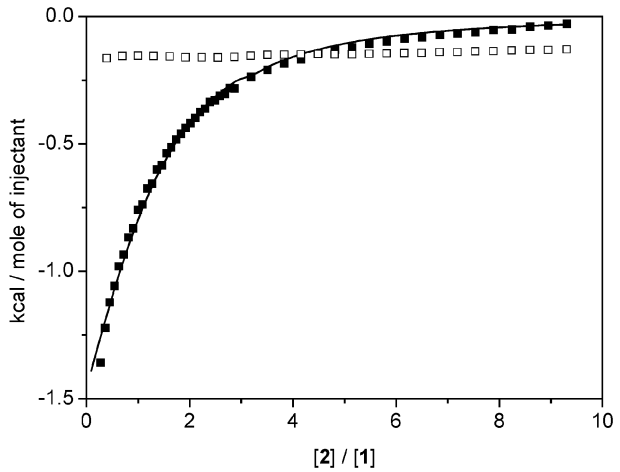


**Fig. 13** ITC titrations of a 200 mM solution of **2** into solvent $CDCl_3$ : MeOD (98 : 2) (□) and into a solution containing 5.0 mM **1** and 50 mM LiI (■) and the fit to a 1 : 1 binding model (solid line).

## Conclusions

These pseudorotaxanes are selective towards small, singly charged cations with geometrically undemanding s orbitals (*i.e.*, $Li^+$ and $Na^+$). The arrangement of the aromatic stacking is parallel for lithium complexes and perpendicular (or highly distorted parallel) for sodium complexes. Use of extremely bulky anions induces steric constraints and modifies the relative donor-acceptor geometry. Lithium cations fit precisely into the pre-organised tetraethylene glycol cavities, whereas the larger sodium cation sits outside the plane formed by the oxygen atoms of the donor and acceptor centres. In addition, solubility of salts also influences the selectivity of the pseudorotaxane. In the case of NaI, formation of a mono-NaI complex was observed as an intermediate.

From a synthetic viewpoint, lithium cations represent ideal templates that could be employed in the formation of rotaxanes and catenanes. The lithium templated pseudorotaxane has ideal properties for the incorporation of this unit into supramolecular devices.

## Experimental

### Methods

$^1H$ and $^{13}C$ NMR spectra were recorded on a Bruker Avance 500 MHz spectrometer using the residual $^1H$ of the deuterated solvent as a reference. The pulse sequence used for 1D NOESY experiments was selnogp.2.[68] UV-Vis spectra were recorded on Hewlett-Packard 8452A diode array spectrometer. All UV-Vis samples were prepared in freshly distilled $CH_2Cl_2$ and recorded at 25 °C. Isothermal titration calorimetry experiments were performed using a MCS Isothermal Titration Microcalorimeter (Microcal Inc. Northampton, MA, USA). Host–guest titrations were corrected for heat of dilution of the syringe contents by subtracting blank titrations into solvent ($CHCl_3$ : MeOH 98 : 2).

### General procedure for the formation of the cation templated pseudorotaxanes

To the 5.0 mM solutions of crown ether **1** (3.2 mg, 5.5 μmol, in $CH_2Cl_2$ or $CHCl_3$ : MeOH 98 : 2), the solid aromatic diimide **2** (1.92 mg, 5.5 μmol) was added. In each case, alkali metal halides (anhydrous) were added in excess (as *ca.* 20 mM solutions in $CH_2Cl_2$ or $CHCl_3$ : MeOH 98 : 2). The suspensions were sonicated for 30–60 s. The time the metal halides were exposed to the atmosphere was kept to the absolute minimum since the salts are extremely hygroscopic. When the salts $LiB(C_6F_5)_4$ and $NaB[3,5\text{-}(CF_3)_2(C_6H_3)]_4$ were used, manipulations were carried out under an atmosphere of $N_2$ prior to product formation; however, handling of the final product and the NMR experiments were carried out under air and using wet $CD_2Cl_2$. Excess salts were separated by filtration and products isolated in quantitative yield after removal of solvent under reduced pressure.

### Crystal structure determination

Crystals were isolated by filtration and a specimen crystal selected under an inert atmosphere, covered with polyfluoroether, and mounted on the end of a nylon loop. Crystal data are summarised in Table 3.†

† CCDC reference numbers 254110–254114. See http://www.rsc.org/suppdata/nj/b4/b415418e/ for crystallographic data in .cif or other electronic format.

Data for complexes $[Li_2 \cdot \mathbf{1} \cdot \mathbf{2}]Br_2$, $[Li_2 \cdot \mathbf{1} \cdot \mathbf{2}][B(C_6F_5)_4]_2$, $[Na_2 \cdot \mathbf{1} \cdot \mathbf{2}]I_2$ and $[Na_2 \cdot \mathbf{1} \cdot \mathbf{2}][B\{3,5\text{-}(CF_3)_2(C_6H_3)\}_4]_2$ were collected at 180 K on a Nonius KappaCCD with graphite-monochromated Mo-K$\alpha$ radiation ($\lambda$ = 0.710 73 Å), as summarised in Table 5. The images were processed with the DENZO and SCALEPACK programs.[74] Crystals of $[Li_2 \cdot \mathbf{1} \cdot \mathbf{2}]I_2$ were small and weakly diffracting, so a synchrotron radiation source was used to collect diffraction data for this compound (at 150 K). Data was collected at Station 9.8, Daresbury SRS, UK, using a Bruker SMART CCD diffractometer. The structures were solved by direct methods using the program SIR92.[75] The refinement and graphical calculations were performed using the CRYSTALS[76,77] and CAMERON[78] software packages. The structures were refined by full-matrix least-squares procedure on *F*. All non-hydrogen atoms were refined with anisotropic displacement parameters. Hydrogen atoms were located in Fourier maps and their positions adjusted geometrically (after each cycle of refinement) with isotropic thermal parameters. Chebychev weighting schemes and empirical absorption corrections were applied.[79]

For complex $[Na_2 \cdot \mathbf{1} \cdot \mathbf{2}][B\{3,5\text{-}(CF_3)_2(C_6H_3)\}_4]_2$, treatment of 3.5 molecules of $H_2O$ (disordered) per asymmetric unit was performed using the procedure described by Spek[80] implemented in PLATON.[81] Structure contains solvent accessible voids of 265.00 $A^3$, equivalent to *ca.* 3.5 molecules of $H_2O$ per asymmetric unit. Identification of the crystallising solvent as water is based upon additional chemical evidence from $^1H$ NMR. Each of the eight $CF_3$ groups has been modelled as disordered over two sites with refined occupancies. In view of the severe shortage of data their temperature factors have been refined isotropically. One hexyl chain has been modelled as disordered over two sites with refined occupancy and isotropic temperature factors.



## Acknowledgements

We thank the Royal Society for a University Research Fellowship (SO) and BBSRC, EPSRC, AstraZeneca and GSK for financial support.

## References

1 J. M. Lehn, *Supramolecular Chemistry Concepts and Perspectives*, VCH, New York, 1995.
2 C. Dietrich-Buchecker, G. Rapenne and J.-P. Sauvage, *Molecular Catenanes, Rotaxanes, and Knots: a Journey through the World of Molecular Topology*, Wiley-VCH, New York, 1999.
3 T. J. Hubin and D. H. Busch, *Coord. Chem. Rev.*, 2000, **200**, 5.
4 C. Reuter, R. Schmieder and F. Vogtle, *Pure Appl. Chem.*, 2000, **72**, 2233.
5 A. R. Pease, J. O. Jeppesen, J. F. Stoddart, Y. Luo, C. P. Collier and J. R. Heath, *Acc. Chem. Res.*, 2001, **34**, 433.
6 K. Kim, *Chem. Soc. Rev.*, 2002, **31**, 96.
7 L. Raehm, D. G. Hamilton and J. K. M. Sanders, *Synlett.*, 2002, 1743.
8 S. J. Rowan, S. J. Cantrill, G. R. L. Cousins, J. K. M. Sanders and J. F. Stoddart, *Angew. Chem., Int. Ed.*, 2002, **41**, 898.
9 V. Balzani, *Photochem. Photobiol. Sci.*, 2003, **2**, 459.
10 M. J. Gunter, *Eur. J. Org. Chem.*, 2004, 1655.
11 J. O. Jeppesen, K. A. Nielsen, J. Perkins, S. A. Vignon, A. Di Fabio, R. Ballardini, M. T. Gandolfi, M. Venturi, V. Balzani, J. Becher and J. F. Stoddart, *Chem.-Eur. J.*, 2003, **9**, 2982.
12 H. R. Tseng, S. A. Vignon and J. F. Stoddart, *Angew. Chem., Int. Ed.*, 2003, **42**, 1491.
13 M. Asakawa, G. Brancato, M. Fanti, D. A. Leigh, T. Shimizu, A. M. Z. Slawin, J. K. Y. Wong, F. Zerbetto and S. W. Zhang, *J. Am. Chem. Soc.*, 2002, **124**, 2939.
14 A. Harada, *Acc. Chem. Res.*, 2001, **34**, 456.
15 V. Balzani, A. Credi, G. Mattersteig, O. A. Matthews, F. M. Raymo, J. F. Stoddart, M. Venturi, A. J. P. White and D. J. Williams, *J. Org. Chem.*, 2000, **65**, 1924.
16 C. P. Collier, J. O. Jeppesen, Y. Luo, J. Perkins, E. W. Wong, J. R. Heath and J. F. Stoddart, *J. Am. Chem. Soc.*, 2001, **123**, 12632.
17 Y. Luo, C. P. Collier, J. O. Jeppesen, K. A. Nielsen, E. Delonno, G. Ho, J. Perkins, H. R. Tseng, T. Yamamoto, J. F. Stoddart and J. R. Heath, *ChemPhysChem*, 2002, **3**, 519.
18 M. R. Diehl, D. W. Steuerman, H. R. Tseng, S. A. Vignon, A. Star, P. C. Celestre, J. F. Stoddart and J. R. Heath, *ChemPhysChem*, 2003, **4**, 1335.
19 C. Wu, M. C. Bheda, C. Lim, X. S. Ya, J. Sze and H. W. Gibson, *Polym. Commun.*, 1991, **32**, 204.
20 J. P. Sauvage and M. Ward, *Inorg. Chem.*, 1991, **30**, 3869.
21 H. W. Gibson, M. Bheda, P. T. Engen, Y. X. Shen, J. Sze, C. Wu, S. Joardar, T. C. Ward and P. R. Lecavalier, *Makromol. Chem., Macromol. Symp.*, 1991, **42–43**, 395.
22 J.-P. Collin, C. Dietrich-Buchecker, P. Gavina, M. C. Jimenez-Molero and J.-P. Sauvage, *Acc. Chem. Res.*, 2001, **34**, 477.
23 M. C. Jimenez, C. O. Dietrich-Buchecker and J.-P. Sauvage, *Angew. Chem., Int. Ed.*, 2000, **39**, 3284.
24 A. M. Brouwer, C. Frochot, F. G. Gatti, D. A. Leigh, L. Mottier, F. Paolucci and G. W. H. Wurpel, *Science*, 2001, **291**, 2124.
25 D. B. Amabilino, P. R. Ashton, L. Perezgarcia and J. F. Stoddart, *Angew. Chem., Int. Ed. Engl.*, 1995, **34**, 2378.
26 F. M. Raymo and J. F. Stoddart, *Pure Appl. Chem.*, 1997, **69**, 1987.
27 F. M. Raymo, K. N. Houk and J. F. Stoddart, *J. Am. Chem. Soc.*, 1998, **120**, 9318.
28 M. Asakawa, P. R. Ashton, V. Balzani, A. Credi, C. Hamers, G. Mattersteig, M. Montalti, A. N. Shipway, N. Spencer, J. F. Stoddart, M. S. Tolley, M. Venturi, A. J. P. White and D. J. Williams, *Angew. Chem., Int. Ed.*, 1998, **37**, 333.
29 S. J. Rowan and J. F. Stoddart, *Org. Lett.*, 1999, **1**, 1913.
30 P. R. Ashton, V. Balzani, J. Becher, A. Credi, M. C. T. Fyfe, G. Mattersteig, S. Menzer, B. N. Mogens, F. M. Raymo, J. F. Stoddart, M. Venturi and D. J. Williams, *J. Am. Chem. Soc.*, 1999, **121**, 3951.
31 P. R. Ashton, R. Ballardini, V. Balzani, A. Credi, K. R. Dress, E. Ishow, C. J. Kleverlaan, O. Kocian, J. A. Preece, N. Spencer, J. F. Stoddart and S. Wenger, *Chem.-Eur. J.*, 2000, **6**, 3558.
32 V. Balzani, A. Credi, G. Mattersteig, O. A. Matthews, F. M. Raymo, J. F. Stoddart, M. Venturi, A. J. P. White and D. J. Williams, *J. Org. Chem.*, 2000, **65**, 1924.
33 A. R. Pease, J. O. Jeppesen, J. F. Stoddart, Y. Luo, C. P. Collier and J. R. Heath, *Acc. Chem. Res.*, 2001, **34**, 433.
34 J. O. Jeppesen, J. Perkins, J. Becher and J. F. Stoddart, *Angew. Chem., Int. Ed.*, 2001, **40**, 1216.
35 H. B. Yu, Y. Luo, K. Beverly, J. F. Stoddart, H. R. Tseng and J. R. Heath, *Angew. Chem., Int. Ed.*, 2003, **42**, 5706.
36 V. Balzani, M. Clemente-Leon, A. Credi, J. N. Lowe, J. D. Badjic, J. F. Stoddart and D. J. Williams, *Chem.-Eur. J.*, 2003, **9**, 5348.
37 M. Alvaro, B. Ferrer, H. Garcia, E. J. Palomares, V. Balzani, A. Credi, M. Venturi, J. F. Stoddart and S. Wenger, *J. Phys. Chem. B*, 2003, **107**, 14319.
38 J. D. Badjic, V. Balzani, A. Credi, S. Silvi and J. F. Stoddart, *Science*, 2004, **303**, 1845.
39 K. S. Chichak, S. J. Cantrill, A. R. Pease, S. H. Chiu, G. W. V. Cave, J. L. Atwood and J. F. Stoddart, *Science*, 2004, **304**, 1308.
40 R. Hernandez, H. R. Tseng, J. W. Wong, J. F. Stoddart and J. I. Zink, *J. Am. Chem. Soc.*, 2004, **126**, 3370.
41 J. O. Jeppesen, C. P. Collier, J. R. Heath, Y. Luo, K. A. Nielsen, J. Perkins, J. F. Stoddart and E. Wong, *J. Phys. IV*, 2004, **114**, 511.
42 S. S. Kang, S. A. Vignon, H. R. Tseng and J. F. Stoddart, *Chem.-Eur. J.*, 2004, **10**, 2555.
43 Y. Liu, A. H. Flood and J. F. Stoddart, *J. Am. Chem. Soc.*, 2004, **126**, 9150.
44 H. R. Tseng, D. M. Wu, N. X. L. Fang, X. Zhang and J. F. Stoddart, *ChemPhysChem*, 2004, **5**, 111.
45 S. A. Vignon, J. Wong, H. R. Tseng and J. F. Stoddart, *Org. Lett.*, 2004, **6**, 1095.
46 E. Baranoff, K. Griffiths, J.-P. Collin, J.-P. Sauvage, B. Ventura and L. Flamigni, *New J. Chem.*, 2004, **28**, 1091.
47 M. Venturi, S. Dumas, V. Balzani, J. Cao and J. F. Stoddart, *New J. Chem.*, 2004, **28**, 1032.
48 D. G. Hamilton, N. Feeder, L. Prodi, S. J. Teat, W. Clegg and J. K. M. Sanders, *J. Am. Chem. Soc.*, 1998, **120**, 1096.
49 D. G. Hamilton, N. Feeder, S. J. Teat and J. K. M. Sanders, *New J. Chem.*, 1998, **22**, 1019.
50 D. G. Hamilton, J. E. Davies, L. Prodi and J. K. M. Sanders, *Chem.-Eur. J.*, 1998, **4**, 608.
51 Q. Zhang, D. G. Hamilton, N. Feeder, S. J. Teat and J. K. M. Sanders, *New J. Chem.*, 1999, **23**, 897.
52 J. G. Hansen, N. Feeder, D. G. Hamilton, M. J. Gunter, J. Becher and J. K. M. Sanders, *Org. Lett.*, 2000, **2**, 449.

53 G. Kaiser, T. Jarrosson, S. Otto, Y.-F. Ng, A. D. Bond and J. K. M. Sanders, *Angew. Chem., Int. Ed.*, 2004, **43**, 1959.
54 T. Iijima, S. A. Vignon, H.-R. Tseng, T. Jarrosson, J. K. M. Sanders, F. Marchioni, M. Venturi, E. Apostoli and J. F. Stoddart, *Chem.-Eur. J.*, 2004, **10**, 6375.
55 F. H. Huang, J. W. Jones, C. Slebodnick and H. W. Gibson, *J. Am. Chem. Soc.*, 2003, **125**, 14458.
56 For the bis-NaI complex, $H_1$ and $H_2$ have NOEs to $NCH_2CH_2$ > $NCH_2$ > $N(CH_2)_2CH_2$, $H_1$ has small NOE to upfield glycol protons, whereas $H_2$ sees the most downfield-shifted $OCH_2CH_2$ proton. $H_3$ has strong NOEs to glycol loops $OCH_2CH_2$ and $H_4$ has three small NOEs to $OCH_2CH_2$ protons. However, the small NOEs could also be interpreted as transfer NOEs of the mono-NaI complex, introduced *via* exchange between the mono- and bis-NaI complexes.
57 B. Cabezon, J. Cao, F. M. Raymo, J. F. Stoddart, A. J. P. White and D. J. Williams, *Angew. Chem., Int. Ed.*, 2000, **39**, 148.
58 P. R. Ashton, E. J. T. Chrystal, J. P. Mathias, K. P. Parry, A. M. Z. Slawin, N. Spencer, J. F. Stoddart and D. J. Williams, *Tetrahedron Lett.*, 1987, **28**, 6367.
59 P. R. Ashton, S. E. Boyd, A. Brindle, S. J. Langford, S. Menzer, L. Perez-Garcia, J. A. Preece, F. M. Raymo, N. Spencer, J. F. Stoddart, A. J. P. White and D. J. Williams, *New J. Chem.*, 1999, **23**, 587.
60 P. R. Ashton, R. Ballardini, V. Balzani, M. Gomez-Lopez, S. E. Lawrence, M. V. Martinez-Diaz, M. Montalti, A. Piersanti, L. Prodi, J. F. Stoddart and D. J. Williams, *J. Am. Chem. Soc.*, 1997, **119**, 10641.
61 P. R. Ashton, O. A. Matthews, S. Menzer, F. M. Raymo, N. Spencer, J. F. Stoddart and D. J. Williams, *Liebigs Ann. Recl.*, 1997, 2485.
62 P. R. Ashton, S. E. Boyd, C. G. Claessens, R. E. Gillard, S. Menzer, J. F. Stoddart, M. S. Tolley, A. J. P. White and D. J. Williams, *Chem.-Eur. J.*, 1997, **3**, 788.
63 H. R. Tseng, S. A. Vignon, P. C. Celestre, J. F. Stoddart, A. J. P. White and D. J. Williams, *Chem.-Eur. J.*, 2003, **9**, 543.
64 P. R. Ashton, S. E. Boyd, S. Menzer, D. Pasini, F. M. Raymo, N. Spencer, J. F. Stoddart, A. J. P. White, D. J. Williams and P. G. Wyatt, *Chem.-Eur. J.*, 1998, **4**, 299.
65 P. R. Ashton, V. Balzani, A. Credi, O. Kocian, D. Pasini, L. Prodi, N. Spencer, J. F. Stoddart, M. S. Tolley, M. Venturi, A. J. P. White and D. J. Williams, *Chem.-Eur. J.*, 1998, **4**, 590.
66 D. G. Hamilton, J. K. M. Sanders, J. E. Davies, W. Clegg and S. J. Teat, *Chem. Commun.*, 1997, 897.
67 P. R. Ashton, R. Ballardini, V. Balzani, A. Credi, M. T. Gandolfi, S. Menzer, L. Perez-Garcia, L. Prodi, J. F. Stoddart, M. Venturi, A. J. P. White and D. J. Williams, *J. Am. Chem. Soc.*, 1995, **117**, 11171.
68 1D NOESY using selective excitation with a shaped pulse; dipolar coupling may be due to NOE or chemical exchange. Pulse sequence used: selnogp.2 (Bruker, advanced version 00/02/07).
69 A. Kumar, G. Wagner, R. R. Ernst and K. Wuthrich, *J. Am. Chem. Soc.*, 1981, **103**, 3654.
70 K. Stott, J. Stonehouse, J. Keeler, T.-L. Hwang and A. J. Shaka, *J. Am. Chem. Soc.*, 1995, **117**, 4199.
71 C. Naumann, B. O. Patrick and J. C. Sherman, *Tetrahedron*, 2002, **58**, 787.
72 For $[Li_2 \cdot \mathbf{1} \cdot \mathbf{2}]I_2$ the rate of dissociation was also determined in a mixture of $CDCl_3$ and MeOD (98 : 2). At 250 K, $k_{-1}$ was 2.3 $s^{-1}$. An Eyring plot was obtained to calculate activation parameters for the formation of the $[Li_2 \cdot \mathbf{1} \cdot \mathbf{2}]I_2$ complex in $CDCl_3$ : MeOD (98 : 2) within the temperature range 230–265 K. The free activation energy is 15.6 $kJ \cdot mmol^{-1}$ lower than that of $[Li_2 \cdot \mathbf{1} \cdot \mathbf{2}]I_2$ formation in $CH_2Cl_2$. Therefore $[Li_2 \cdot \mathbf{1} \cdot \mathbf{2}]I_2$ is less stable kinetically in the more polar medium. Using relative rates is an illustrative way to describe kinetic differences. For example, in the case of the LiI complex, the dissociation/association process takes place 24 000 times faster in $CDCl_3$ : MeOD (98 : 2) than in $CD_2Cl_2$!.
73 J. W. Jones and H. W. Gibson, *J. Am. Chem. Soc.*, 2003, **125**, 7001.
74 Z. Otwinowski and W. Minor, in *Methods in Enzymology*, eds. C. N. Carter, Jr. and R. M. Sweet, Academic Press, London, 1996.
75 A. Altomare, G. Carascano, C. Giacovazzo and A. Guagliardi, *J. Appl. Crystallogr.*, 1993, **26**, 343.
76 D. J. Watkin, C. K. Prout, J. R. Carruthers and P. W. Betteridge, *CRYSTALS*, Oxford, UK, 1996.
77 P. W. Betteridge, J. R. Carruthers, R. I. Cooper, K. Prout and D. J. Watkin, *J. Appl. Crystallogr.*, 2003, **36**, 1487.
78 D. J. Watkin, C. K. Prout and L. J. Pearce, *CAMERON*, Oxford, UK, 1996.
79 N. Walker and D. Stuart, *Acta Crystallogr., Sect. A*, 1983, **39**, 158.
80 A. L. Spek, *J. Appl. Crystallogr.*, 2003, **36**, 7.
81 A. L. Spek, *PLATON, A Multipurpose Crystallographic Tool*, Utrecht, The Netherlands, 1998.